



## Technical Notes

Preparation and characterization of  $^{33}\text{S}$  samples for  $^{33}\text{S}(n,\alpha)^{30}\text{Si}$  cross-section measurements at the n\_TOF facility at CERN

J. Praena<sup>1,\*</sup>, F.J. Ferrer<sup>2</sup>, W. Vollenberg<sup>3</sup>, M. Sabaté-Gilarte<sup>4,3</sup>, B. Fernández<sup>2,4</sup>, J. García-López<sup>2,4</sup>, I. Porras<sup>1</sup>, J.M. Quesada<sup>4</sup>, S. Altstadt<sup>5</sup>, J. Andrzejewski<sup>6</sup>, L. Audouin<sup>7</sup>, V. Bécares<sup>8</sup>, M. Barbagallo<sup>9</sup>, F. Bečvář<sup>10</sup>, F. Belloni<sup>11</sup>, E. Berthoumieux<sup>11</sup>, J. Billowes<sup>12</sup>, V. Boccone<sup>3</sup>, D. Bosnar<sup>13</sup>, M. Brugger<sup>3</sup>, F. Calviño<sup>14</sup>, M. Calviani<sup>3</sup>, D. Cano-Ott<sup>8</sup>, C. Carrapiço<sup>15</sup>, F. Cerutti<sup>3</sup>, E. Chiaveri<sup>3,11</sup>, M. Chin<sup>3</sup>, N. Colonna<sup>9</sup>, G. Cortés<sup>14</sup>, M.A. Cortés-Giraldo<sup>4</sup>, M. Diakaki<sup>16</sup>, M. Dietz<sup>17</sup>, C. Domingo-Pardo<sup>18</sup>, R. Dressler<sup>19</sup>, I. Durán<sup>20</sup>, C. Eleftheriadis<sup>21</sup>, A. Ferrari<sup>3</sup>, K. Fraval<sup>11</sup>, V. Furman<sup>22</sup>, K. Göbel<sup>5</sup>, M.B. Gómez-Hornillos<sup>14</sup>, S. Ganesan<sup>23</sup>, A.R. García<sup>8</sup>, G. Giubrone<sup>18</sup>, I.F. Gonçalves<sup>15</sup>, E. González-Romero<sup>8</sup>, A. Goverdovski<sup>24</sup>, E. Griesmayer<sup>25</sup>, C. Guerrero<sup>3</sup>, F. Gunsing<sup>11</sup>, T. Heftrich<sup>5</sup>, A. Hernández-Prieto<sup>3,14</sup>, J. Heyse<sup>26</sup>, D.G. Jenkins<sup>27</sup>, E. Jericha<sup>25</sup>, F. Käppeler<sup>28</sup>, Y. Kadi<sup>3</sup>, D. Karadimos<sup>16</sup>, T. Katabuchi<sup>29</sup>, V. Ketlerov<sup>24</sup>, V. Khryachkov<sup>24</sup>, N. Kivel<sup>19</sup>, P. Koehler<sup>30</sup>, M. Kokkoris<sup>16</sup>, J. Kroll<sup>10</sup>, M. Krtička<sup>10</sup>, C. Lampoudis<sup>11</sup>, C. Langer<sup>5</sup>, E. Leal-Cidoncha<sup>20</sup>, C. Lederer<sup>31</sup>, H. Leeb<sup>25</sup>, L.S. Leong<sup>7</sup>, J. Lerendegui-Marco<sup>4</sup>, R. Losito<sup>3</sup>, A. Mallick<sup>23</sup>, A. Manousos<sup>21</sup>, J. Marganiec<sup>6</sup>, T. Martínez<sup>8</sup>, C. Massimi<sup>32,33</sup>, P. Mastinu<sup>34</sup>, M. Mastromarco<sup>9</sup>, E. Mendoza<sup>8</sup>, A. Mengoni<sup>35</sup>, P.M. Milazzo<sup>36</sup>, F. Mingrone<sup>32</sup>, M. Mirea<sup>37</sup>, W. Mondelaers<sup>26</sup>, C. Paradela<sup>20</sup>, A. Pavlik<sup>31</sup>, J. Perkowski<sup>6</sup>, A.J.M. Plompen<sup>26</sup>, T. Rauscher<sup>38</sup>, R. Reifarh<sup>5</sup>, A. Riego-Perez<sup>14</sup>, M. Robles<sup>20</sup>, C. Rubbia<sup>3</sup>, J.A. Ryan<sup>12</sup>, R. Sarmiento<sup>15</sup>, A. Saxena<sup>23</sup>, P. Schillebeeckx<sup>26</sup>, S. Schmidt<sup>5</sup>, D. Schumann<sup>19</sup>, P. Sedyshev<sup>22</sup>, G. Tagliente<sup>9</sup>, J.L. Tain<sup>18</sup>, A. Tarifeño-Saldivia<sup>18</sup>, D. Tarrío<sup>20</sup>, L. Tassan-Got<sup>7</sup>, A. Tsinganis<sup>3</sup>, S. Valenta<sup>10</sup>, G. Vannini<sup>32,33</sup>, V. Variale<sup>9</sup>, P. Vaz<sup>15</sup>, A. Ventura<sup>32</sup>, M.J. Vermeulen<sup>27</sup>, V. Vlachoudis<sup>3</sup>, R. Vlastou<sup>16</sup>, A. Wallner<sup>39</sup>, T. Ware<sup>12</sup>, M. Weigand<sup>5</sup>, C. Weiss<sup>25</sup>, T. Wright<sup>12</sup>, P. Žugec<sup>13</sup>, The n\_TOF Collaboration<sup>1</sup>

<sup>1</sup> Universidad de Granada, Spain<sup>2</sup> Centro Nacional de Aceleradores, Sevilla, Spain<sup>3</sup> European Organization for Nuclear Research (CERN), Switzerland<sup>4</sup> Universidad de Sevilla, Spain<sup>5</sup> Goethe University Frankfurt, Germany<sup>6</sup> University of Lodz, Poland<sup>7</sup> Institut de Physique Nucléaire, CNRS-IN2P3, Univ. Paris-Sud, Université Paris-Saclay, F-91406 Orsay Cedex, France<sup>8</sup> Centro de Investigaciones Energéticas Medioambientales y Tecnológicas (CIEMAT), Spain<sup>9</sup> Istituto Nazionale di Fisica Nucleare, Sezione di Bari, Italy<sup>10</sup> Charles University, Prague, Czech Republic<sup>11</sup> CEA Irfu, Université Paris-Saclay, F-91191 Gif-sur-Yvette, France<sup>12</sup> University of Manchester, United Kingdom<sup>13</sup> Department of Physics, Faculty of Science, University of Zagreb, Zagreb, Croatia<sup>14</sup> Universitat Politècnica de Catalunya, Spain<sup>15</sup> Instituto Superior Técnico, Lisbon, Portugal<sup>16</sup> National Technical University of Athens, Greece<sup>17</sup> School of Physics and Astronomy, University of Edinburgh, United Kingdom

\* Corresponding author.

E-mail address: [jpraena@ugr.es](mailto:jpraena@ugr.es) (J. Praena).<sup>1</sup> <http://www.cern.ch/ntof>.

<sup>18</sup> Instituto de Física Corpuscular, Universidad de Valencia, Spain<sup>19</sup> Paul Scherrer Institut (PSI), Villigen, Switzerland<sup>20</sup> University of Santiago de Compostela, Spain<sup>21</sup> Aristotle University of Thessaloniki, Thessaloniki, Greece<sup>22</sup> Joint Institute for Nuclear Research (JINR), Dubna, Russia<sup>23</sup> Bhabha Atomic Research Centre (BARC), India<sup>24</sup> Institute of Physics and Power Engineering (IPPE), Obninsk, Russia<sup>25</sup> Technische Universität Wien, Austria<sup>26</sup> European Commission, Joint Research Centre, Geel, Retieseweg 111, B-2440 Geel, Belgium<sup>27</sup> University of York, United Kingdom<sup>28</sup> Karlsruhe Institute of Technology, Campus North, IKP, 76021 Karlsruhe, Germany<sup>29</sup> Tokyo Institute of Technology, Japan<sup>30</sup> Oak Ridge National Laboratory (ORNL), Oak Ridge, TN 37831, USA<sup>31</sup> University of Vienna, Faculty of Physics, Vienna, Austria<sup>32</sup> Istituto Nazionale di Fisica Nucleare, Sezione di Bologna, Italy<sup>33</sup> Dipartimento di Fisica e Astronomia, Università di Bologna, Italy<sup>34</sup> Istituto Nazionale di Fisica Nucleare, Sezione di Legnaro, Italy<sup>35</sup> Agenzia nazionale per le nuove tecnologie (ENEA), Bologna, Italy<sup>36</sup> Istituto Nazionale di Fisica Nucleare, Sezione di Trieste, Italy<sup>37</sup> Horia Hulubei National Institute of Physics and Nuclear Engineering, Romania<sup>38</sup> Department of Physics, University of Basel, Switzerland<sup>39</sup> Australian National University, Canberra, Australia

## ARTICLE INFO

## Keywords:

Neutron induced alpha emission

Thermal evaporation

Rutherford backscattering

## ABSTRACT

Thin  $^{33}\text{S}$  samples for the study of the  $^{33}\text{S}(n,\alpha)^{30}\text{Si}$  cross-section at the n\_TOF facility at CERN were made by thermal evaporation of  $^{33}\text{S}$  powder onto a dedicated substrate made of kapton covered with thin layers of copper, chromium and titanium. This method has provided for the first time bare sulfur samples a few centimeters in diameter. The samples have shown an excellent adherence with no mass loss after few years and no sublimation in vacuum at room temperature. The determination of the mass thickness of  $^{33}\text{S}$  has been performed by means of Rutherford backscattering spectrometry. The samples have been successfully tested under neutron irradiation.

## 1. Introduction

The preparation of thin sulfur samples is a difficult task because sulfur sublimates in vacuum at room temperature, adheres poorly or only for a short time to most solid backings and it is very volatile [1–4]. These difficulties are enhanced by the particularities required for an accurate study of the  $^{33}\text{S}(n,\alpha)^{30}\text{Si}$  cross-section as a function of the neutron energy. The only two experiments with the goal of the measurement of the  $^{33}\text{S}(n,\alpha)^{30}\text{Si}$  cross-section in a wide energy range reported different problems with the samples [5,6]. Thin deposits are needed for a low energy loss and good detection efficiency of the emitted alpha particles, but at the same time, the value of the cross-section in some energy ranges is expected to be low, therefore an adequate number of atoms per  $\text{cm}^2$  is required. On the other side, the cross-section is expected to be high in the resonance region but for resolving the resonances a pulsed neutron beam is mandatory entailing a decrease of the neutron flux. With all of this in mind and with the knowledge of the outstanding characteristics of the Experimental Area 1 (EAR1) of the n\_TOF-CERN facility in terms of energy resolution and instantaneous flux, it is also possible to take advantage of a higher number of neutrons making use of the beam of 8 cm diameter during the so-called fission campaign when the large collimator is installed [7]. This possibility implies an additional double challenge, the production of large samples and their accurate characterization with an adequate study of the homogeneity.

In spite of these difficulties, some problems have been solved by different authors depending on the requirements of their experiments. Watson developed a technique for making sulfur targets for the purpose of proton capture studies [1]. The target was a thin layer of  $\text{Ag}_2\text{S}$  but only  $10^{-8}$  at/b were present, which is an order of magnitude lower than the requirement for neutron-capture studies as those foreseen at n\_TOF. The same can be concluded for ion-implanted S targets performed by

different authors, as Schatz et al. [4]. That kind of targets has the additional drawback of the small dimensions (2 cm diameter) that in the case of the EAR1 at n\_TOF would mean an important waste of neutrons making impossible this measurement in a reasonable time. Hedemann [2] showed a relatively good adherence of sulfur to formvar foils and made a multi-sandwich target of formvar-carbon-sulfur. However, migration and loss of sulfur was reported. Geerts et al. [3], based on Hedemann's work, produced a  $^{33}\text{S}$  sample using a sandwich of formvar foils. No sulfur losses or migration was reported during an irradiation of the sample with thermal neutrons [3]. As formvar powder is usually diluted in a solution which is classified as dangerous (carcinogenic and toxic) many formvar solutions should be disposed as hazardous waste. Therefore, we decided to avoid using formvar in our work.

All previous methods were based on the evaporation of sulfur in different conditions or ion implantation. There have been more attempts to prepare sulfur samples by deposition from a well-defined solution [4]. However, this method provided samples with significant inhomogeneities requiring large self-absorption corrections.

Regarding uncertainties, the characterization of the samples was carried out by different techniques. In general around  $\pm 20\%$  uncertainty for the number of atoms were obtained, but no information was provided for the homogeneity. In Ref. [4] an accuracy better than  $\pm 20\%$  was obtained, but the adherence before and after the experiment was not investigated and long tails in the alpha spectrum towards lower energies were present due to significant inhomogeneities, which entailed a degradation in separating the alpha-induced signals from the background [4].

In this work, we present a method for making large  $^{33}\text{S}$  samples, stable in vacuum and at atmospheric pressure, with no observable mass loss over a period of few years and without cover layer. An accurate determination of the number of atoms per  $\text{cm}^2$  is also presented. The method is based on the evaporation in vacuum of  $^{33}\text{S}$  powder onto a dedicated substrate and the characterization is based on Rutherford backscattering spectrometry (RBS).

## 2. Preparation and characterization of $^{33}\text{S}$ samples

As already pointed out, the production of  $^{33}\text{S}$  samples for neutron-induced cross-section measurements is not straightforward. In addition to the mentioned factors, it was necessary to avoid the use of materials with elements that under neutron irradiation could produce charged-particles leading to undesirable signals in the spectra. Also, the substrate must be made of a conductive material in order to use the  $n_{\text{TOF}}$  experimental setup based on MICRO MESH Gaseous Structure (Micromegas) detector [8] for taking advantage of its high efficiency, low mass, and high neutron transparency that permits using several in-beam detectors [9].

### 2.1. Sample coating

According to these requirements, several tests of the adhesion of natural sulfur were carried out at the Vacuum, Surfaces and Coating (VSC) group of the Technology Department at CERN. It was found that sulfur showed good adherence to commercially available copper-plated kapton foils at moderate deposition temperature ( $60\text{ }^{\circ}\text{C}$ ). A strong bonding of S and Cu could be achieved due to the formation of a stable compound, similar to the case of S and Ag [1]. The production procedure of the final 6 samples is described in the following.

A commercially available  $50\text{ }\mu\text{m}$  kapton foil with  $25\text{ nm}$  Cr and  $5\text{ }\mu\text{m}$  Cu served as starting material. The Cu thickness was reduced for decreasing possible background from neutron-induced reactions on Cu. To this end, the superficial layer was removed by chemical etching. Then, in a magnetron deposition coating equipment a  $10\text{ nm}$  Titanium adhesion layer and a  $200\text{ nm}$  Cu layer were deposited without intermediate air exposure. Once the substrate was prepared the evaporation of  $^{33}\text{S}$  powder, with an enrichment higher than  $99\%$  [10] was performed in a glass bell jar of  $30\text{ cm}$  in diameter and  $35\text{ cm}$  in height. Few milligrams of powder were loaded in a molybdenum boat (Balzers BD 482 056) with a Mo cover. The central hole of  $5\text{ mm}$  in diameter was positioned at  $11.5\text{ cm}$  from the substrate. The substrate was heated at  $60\text{ }^{\circ}\text{C}$  during  $1\text{ h}$ . The chamber was externally heated during the same time and at the same temperature. The pressure was decreased to  $6\text{--}10^{-4}\text{ mbar}$  with a rotary vane pump by pumping through a cold trap filled with liquid nitrogen ( $\text{LN}_2$ ). The  $^{33}\text{S}$  powder was completely evaporated passing a current of  $70\text{ A}$  through the Mo boat during  $5\text{ min}$ . A collimator ( $9\text{ cm}$  diameter) was used to fit the dimensions of the  $n_{\text{TOF}}$  neutron beam during the EAR1 fission campaign ( $8\text{ cm}$  diameter) and for avoiding possible edge effects. Once the evaporation was finished, the sample and the chamber were kept at  $60\text{ }^{\circ}\text{C}$  during  $1\text{ h}$ .

Fig. 1 shows the substrate before (top) and after (bottom) the evaporation of  $^{33}\text{S}$ . The area in which the  $^{33}\text{S}$  reacted with Cu is clearly noticeable by the dark color formation of a compound between Cu and  $^{33}\text{S}$ . By evaporation of masses of  $^{33}\text{S}$  batches with  $5$  and  $15\text{ mg}$ , six samples of different thicknesses have been produced.

### 2.2. Rutherford backscattering analysis

The samples were characterized at the  $3\text{ MV}$  Tandem Pelletron accelerator at the Centro Nacional de Aceleradores (CNA, Spain). At CNA, an accelerator line is dedicated to different Ion Beam Analysis techniques and in particular RBS [11]. The characterization of the samples was performed with a mono-energetic beam of  $3.5\text{ MeV}$   $^4\text{He}^{++}$ . The scattered  $^4\text{He}$  ions were recorded in a Passivated Implanted Planar Silicon (PIPS) detector of  $300\text{ mm}^2$ , positioned at a scattering angle of  $165^{\circ}$ . For calibration purposes a reference sample containing  $18\cdot 10^{-9}\text{ at/b}$  of Pt deposited over a thick ( $0.5\text{ mm}$ ) Si substrate was used. The sample holder was tilted by  $7^{\circ}$  with respect to the beam direction to avoid channeling effects. In order to perform absolute RBS measurements the number of incident  $\alpha$ -particles must be precisely known. For this purpose and to suppress secondary electrons that can produce false current measurements, the sample holder was electrically isolated and

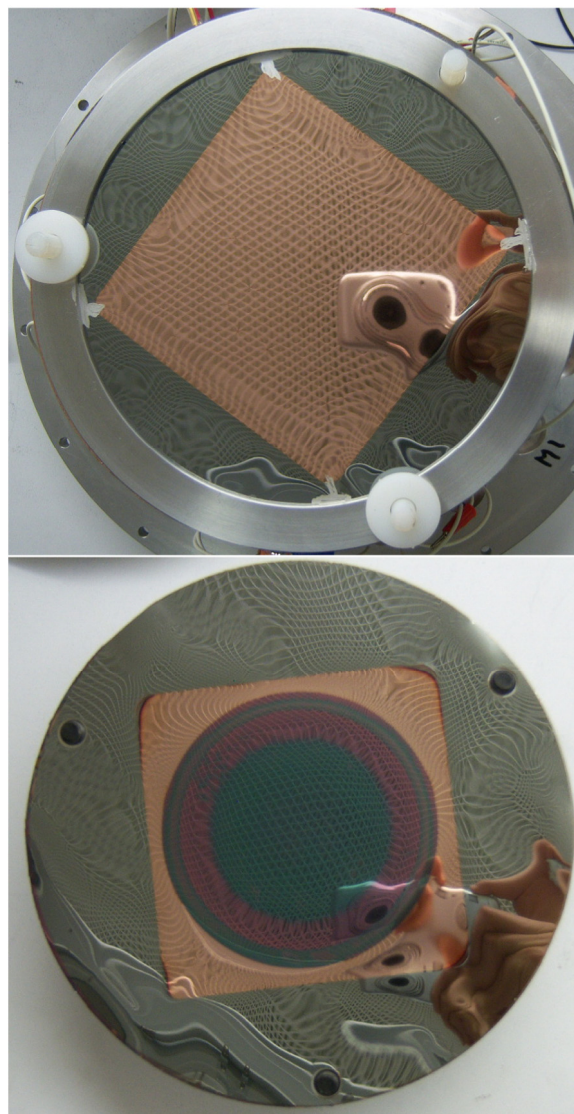
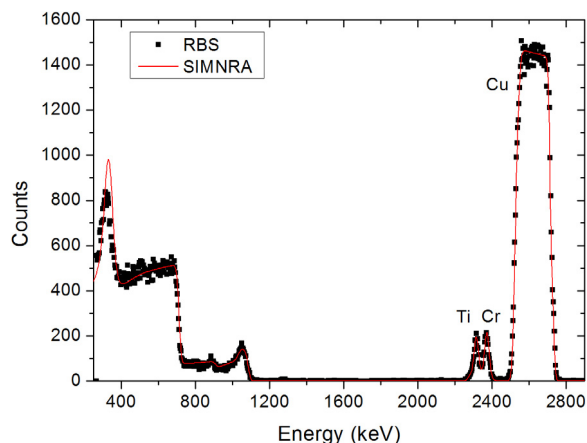


Fig. 1. The sample before the evaporation of  $^{33}\text{S}$  (top) and after the evaporation of  $^{33}\text{S}$  (bottom). The sample on top is what we call substrate and the inner dark area in the photo on the bottom corresponds to the  $^{33}\text{S}$  sample.

was kept at a potential of  $200\text{ V}$  potential, thus acting as a Faraday cup. In this way, the  $\alpha$ -current was measured directly at the sample, which was in contact with the sample holder. In addition, the sample holder is equipped with a XY stage using stepping motors with a precision of  $100\text{ }\mu\text{m}$ . This allowed an accurate positioning of the sample in the beam. The RBS spectra were analyzed using the SIMNRA package [12].

Because of the dimensions of the samples ( $8\text{ cm}$  diameter) and the  $^4\text{He}^{++}$  beam spot ( $3\text{ mm}$ ), several points were analyzed for each sample. The samples were scanned from one edge to other, not in the radial direction, passing through the center. The energy of the  $^4\text{He}^{++}$  was selected at  $3.5\text{ MeV}$  because the scattering cross-section can be chosen as Rutherford and a good separation of the backscattered alphas by the different elements in the sample was achieved. Indeed, the energy of the  $^4\text{He}$ -ion in the center-of-mass ( $E_{cm}$  in MeV) at which the scattering cross-section deviates by  $2\%$  from its Rutherford value vs. atomic number ( $Z$ ) is given by  $E_{cm} = 0.041 + 0.232\cdot Z$  [13]. In case of  $^{33}\text{S}$ , the corresponding energy in the laboratory system is  $4.2\text{ MeV}$  (higher than  $3.5\text{ MeV}$ ). This energy is higher for heavier atoms. Therefore, in our simulations, we will use the Rutherford cross-section for the scattering of  $^4\text{He}^{++}$  in S, Cu, Cr and Ti. For the C, N and O, we will use the





**Fig. 2.** RBS spectrum of the substrate measured using a 3.5 MeV  $^4\text{He}^{++}$  beam. The points correspond to the experimental data and the line to the SIMNRA simulation [12]. From higher to lower energy the peaks correspond to Cu, Cr, Ti and kapton elements; see text for details.

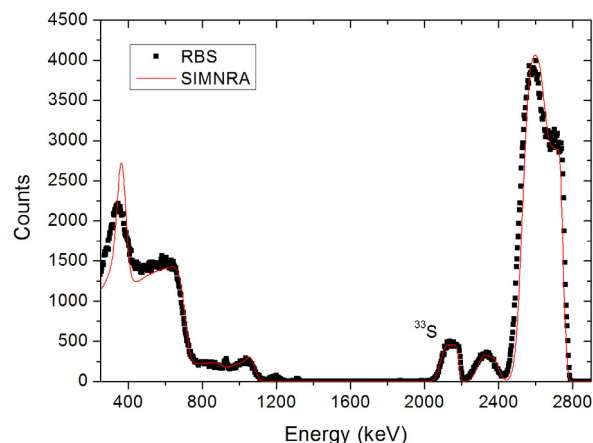


**Fig. 3.** RBS spectrum measured using a 3.5 MeV  $^4\text{He}^{++}$  beam for the  $^{33}\text{S}$  samples. The points correspond to the experimental data and the line to the SIMNRA [12] simulation. From higher energy to lower energy the peaks correspond to Cu, Ti-Cr,  $^{33}\text{S}$  and the elements of the kapton; see text for details.

evaluated (SigmCalc) cross section data from IBANDL database, IAEA, 2014 [14].

In order to perform an accurate and precise determination of the number of atoms of  $^{33}\text{S}$  few points outside the area with sulfur were also analyzed by RBS. This allowed the determination of the number of atoms of the elements present in the substrate reducing the free parameters of the SIMNRA fit of the experimental data. Fig. 2 shows one of these points where the experimental RBS spectrum (black points) is compared with the SIMNRA simulation (red line). The biggest peak from 2500 to 2800 keV corresponds to Cu, the second in energy to Cr and third in energy to Ti. Then, below 1200 keV the different elements present in kapton are detected. The simulation of the area without  $^{33}\text{S}$  provides a very good fit of the experimental data for Cu, Cr and Ti giving their number of atoms in the substrate. Below 500 keV the signals from the lighter elements of kapton are not perfectly fitted. This is due to multiple scattering effects at low energy which are difficult to simulate. Different points of the substrate provided the same values of the number of atoms per unit of area within uncertainty of each element.

Fig. 3 shows a RBS spectrum (black points) in comparison with the SIMNRA simulation (red line) of a point with  $^{33}\text{S}$ . Between 2000 and 2200 keV the  $\alpha$ -particles backscattered by  $^{33}\text{S}$  are clearly detected with a good separation from the rest of elements allowing the determination of the total number of atoms of  $^{33}\text{S}$ . The SIMNRA simulation provides a very good fit of the  $^{33}\text{S}$  peak.

From the comparison between Figs. 2 and 3 other differences could be noticed. The Cr and Ti peaks are not resolved due to the presence of  $^{33}\text{S}$ . This is described by the SIMNRA simulation and the fit of the Cr-Ti peak remains very good. When sulfur is evaporated the Cu peak is split, which means that the  $^{33}\text{S}$  only reacted with a part of the Cu layer in depth. The part of the Cu peak at higher energies corresponds to Cu that reacted with  $^{33}\text{S}$  and the rest of the peak corresponds to the Cu not reacting with  $^{33}\text{S}$ . The latter has a higher number of atoms of Cu per unit of area than the former. Also this fact is described by the SIMNRA simulation.

In order to estimate the uncertainty, several simulations of each point were carried out. Once the experimental data were fitted with SIMNRA, the same simulation was performed varying the number of atoms of  $^{33}\text{S}$ . The result of this study for each point demonstrated that  $\pm 2$ –3% difference in the number of  $^{33}\text{S}$  atoms meant that the peak due to backscattered  $\alpha$ -particles by  $^{33}\text{S}$  was not fitted. Thus, in order to provide a conservative estimation of the accuracy, 3% will be considered as a relative uncertainty of the mass. The process of data taking and fitting the experimental data with the SIMNRA code was performed for all the

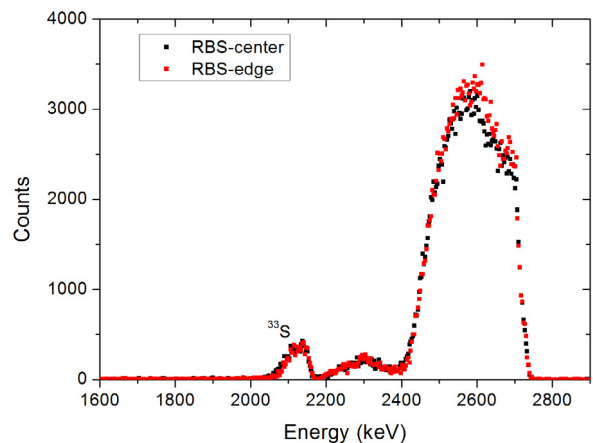


**Fig. 4.** RBS spectra measured using a 3.5 MeV  $^4\text{He}^{++}$  beam. Black points correspond to a point measured at the central area of the sample. Red points correspond to a point measured at 3 cm from the center. (For interpretation of the references to color in this figure legend, the reader is referred to the web version of this article.)

points and samples. At least fifteen points of each sample were analyzed allowing a detailed characterization of the  $^{33}\text{S}$  area. Points at equal distance from the center showed an equal number of atoms per  $\text{cm}^2$  within uncertainties. Statistical uncertainty in the number of  $^{33}\text{S}$  atoms ranges between 3–5% depending on the point. For each sample, the number of atoms of  $^{33}\text{S}$  obtained from each point, normalized to the  $\alpha$ -current, was almost the same, with a maximum difference of  $\pm 4$ –5%. Therefore, we consider the samples as homogeneous with an additional 5% uncertainty in the number of atoms. Fig. 4 shows two RBS spectra of the same sample illustrating its homogeneity. One spectrum (black points) was obtained in the central area of the sample and the other (red points) at 3 cm from the center.

Table 1 summarizes the results for all the samples. The number of atoms per barn corresponds to the calculated total mass divided by the area of the sample for a radius of 4 cm. Several RBS analysis of the samples have been carried out throughout four years. The results of the analysis showed the same values of the number of atoms per barn as Table 1 within uncertainties.

**Table 1**  
Results of the number of atoms of  $^{33}\text{S}$  per barn for all the samples.

	$\cdot 10^{-7}(\text{at/b})$	$\pm$ Uncertainty
Sample 1	3.79	0.31
Sample 2	3.49	0.28
Sample 3	2.59	0.23
Sample 4	2.15	0.20
Sample 5	3.76	0.31
Sample 6	3.65	0.29

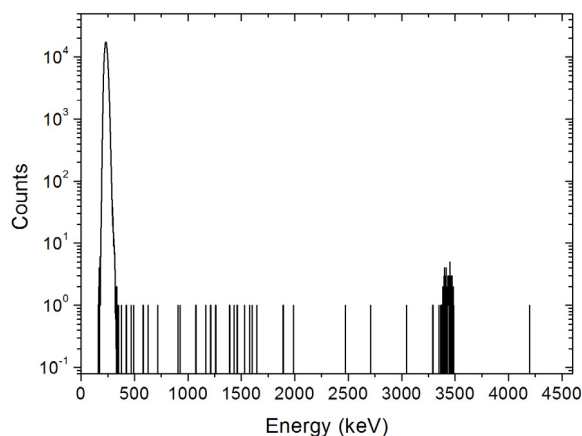


**Fig. 5.** Pulse-height distribution in energy of one  $^{33}\text{S}$  sample under neutron irradiation. Signals at 3.4 MeV correspond to the  $\alpha$ -particles from the  $^{33}\text{S}(n,\alpha)^{30}\text{Si}$  reaction.

### 3. Performance of the samples under neutron irradiation

The  $^{33}\text{S}(n,\alpha)^{30}\text{Si}$  reaction has a  $Q$ -value equal to 3493 keV with no threshold [15]. Therefore,  $\alpha$ -particles of around 3.4 MeV can be detected under the irradiation with low energy neutrons. In this way, the performance of the samples for future experiments can be tested. At CNA, an accelerator-based neutron source has been developed. In particular, neutron beams practically following a Maxwell-Boltzmann distribution are produced for astrophysics studies [16] [17]. The energy spectrum of such beams has its maximum probability at 30 keV. The neutron flux can reach up to  $10^8 \text{ n s}^{-1} \text{ cm}^{-2}$ , which is adequate for a test of the samples under neutron irradiation. The details of the neutron production method can be found in [16,17].

Sample 1 was irradiated with a neutron field similar to a Maxwellian at  $kT=30 \text{ keV}$  and the emitted alpha particles were detected with a setup consisting of three PIPS detectors ( $500 \mu\text{m}$ ). The distance from the sample to the neutron target was 3 cm and 4 cm from the sample to the PIPS. Fig. 5 shows a pulse-height spectrum obtained during the irradiation. The signals between 3.4–3.5 MeV correspond to the alpha particles produced in the  $^{33}\text{S}(n,\alpha)^{30}\text{Si}$  reaction, which shows that the energy of the  $\alpha$ -particles is not significantly degraded by the sample. Other signals correspond to electronic noise.

A second test was carried out at the Experimental Area 1 of the n\_TOF-CERN facility. One  $^{33}\text{S}$  sample and one sample without  $^{33}\text{S}$  (see top photo in Fig. 1), were setup in the usual configuration of Micromegas detectors at n\_TOF [9,18]. The signals detected by the Micromegas as a function of the time are shown in Fig. 6. Blue line corresponds to the detector with  $^{33}\text{S}$  and red line to the detector without  $^{33}\text{S}$ . Both detectors registered very low amplitude signals corresponding to noise and background forming the so called baseline. One large negative amplitude signal is shown in the detector with  $^{33}\text{S}$ , which corresponds to an  $\alpha$ -particle. During the test, many signals with large amplitude were detected in the Micromegas with  $^{33}\text{S}$ , meanwhile no signals with amplitude larger than the baseline were detected in the detector without  $^{33}\text{S}$ . Therefore, the test shows the adequate selection of the substrate because of the lack of signals that could contaminate those due to the  $^{33}\text{S}(n,\alpha)^{30}\text{Si}$  reaction.

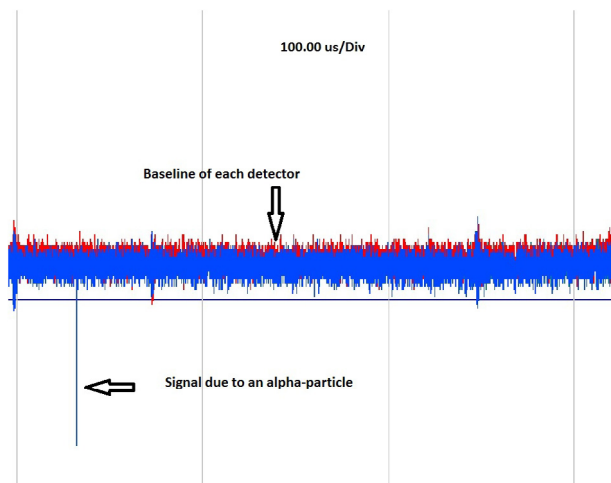


**Fig. 6.** Snapshot of the signals registered by two Micromegas detectors, one with  $^{33}\text{S}$  (blue line) and one without  $^{33}\text{S}$  (red line). It can be clearly seen a signal from an  $\alpha$ -particle below the baseline in the detector with  $^{33}\text{S}$ . (For interpretation of the references to color in this figure legend, the reader is referred to the web version of this article.)

### 4. Conclusions

Six samples of  $^{33}\text{S}$  were produced at VSC-CERN for  $^{33}\text{S}(n,\alpha)^{30}\text{Si}$  cross-section measurements at the n\_TOF-CERN facility. The characterization by RBS performed at CNA has allowed an accurate determination (around 9% of uncertainty) of the number of  $^{33}\text{S}$  atoms per unit of area present in the samples. From 2012 to present, the samples have been stored the major part of the time in a clean laboratory with normal air. During the different experiments presented in this work they were in high vacuum ( $10^{-6} \text{ mbar}$ ). Under these conditions the samples have shown an excellent stability with no loss of mass. This was checked by means of several RBS analysis of the samples throughout these years. Therefore, we can conclude that for first time stable bare  $^{33}\text{S}$  samples of large dimensions have been produced for  $^{33}\text{S}(n,\alpha)^{30}\text{Si}$  cross-section measurements. The developed method provides quasi homogeneous samples and avoids the sublimation of  $^{33}\text{S}$  in vacuum at room temperature. The tests carried out at CNA and CERN demonstrated the good performance of the samples for future experiments with the aim of measuring the  $^{33}\text{S}(n,\alpha)^{30}\text{Si}$  cross-section.

### Acknowledgments

This work was supported by the Spanish projects FPA2013-47327-C2-1-R, FPA2014-53290-C2-2-P, FPA2016-77689-C2-1-R, J. de Andalucía P11-FQM-8229, FIS2015-69941-C2-1-P (MINECO-FEDER, EU), AECC-PS16163811PORR and the funding agencies of the participating institutes. The authors are grateful to J.A. Labrador and A. Romero for the high quality of the beam at CNA.

### References

- [1] D.D. Watson, Simple method for making sulfur targets, *Rev. Sci. Instr.* 37 (1966) 1605.
- [2] M.A. Hedemann, Preparation of isotopic sulfur targets, *Nucl. Instrum. Methods Phys. Res. A* 141 (1977) 377–379.
- [3] K. Geerts, J. van Gestel, J. Pauwels, Thin  $^{33}\text{S}$  layers for  $^{33}\text{S}(n,\alpha)$  cross-section measurements, *Nucl. Instrum. Methods Phys. Res. A* 236 (1985) 527–529.
- [4] H. Schatz, S. Jaag, G. Linker, R. Steininger, F. Käppeler, P.E. Koehler, S.M. Graff, M. Wiescher, Stellar cross sections for  $^{33}\text{S}(n,\alpha)^{30}\text{Si}$ ,  $^{36}\text{Cl}(n,p)^{36}\text{S}$  and  $^{36}\text{Cl}(n,\alpha)^{33}\text{P}$  and the origin of the  $^{36}\text{S}$ , *Phys. Rev. C* 51 (1) (1995) 379.
- [5] G.F. Auchampaugh, J. Halperin, R.L. Macklin, W.M. Howard, Kilovolt  $^{33}\text{S}(n,\alpha)$  and  $^{33}\text{S}(n,\gamma)$  cross sections: Importance in the nucleosynthesis of the rare nucleus  $^{36}\text{S}$ , *Phys. Rev. C* 12 (1975) 1126–1133.

- [6] C. Wagemans, H. Weigmann, R. Barthelemy, Nuclear Phys. A 469 (1987) 497–506.
- [7] C. Guerrero, A. Tsinganis, E. Berthoumieux, et al., The n\_TOF Collaboration, Performance of the neutron time-of-flight facility n\_TOF at CERN, Eur. Phys. J. A 49 (2013) 17.
- [8] G. Charpak, Y. Giomataris, J. Derr, Ph. Rebourgeard, Micromegas, a multipurpose gaseous detector, Nucl. Instrum. Methods Phys. Res. A 478 (2002) 26–36.
- [9] S. Andriamonje, et al., J. Korean Phys. Soc. 59 (2011) 1597–1600.
- [10] Trace Science International. <http://www.tracesciences.com/index.html>.
- [11] J. García López, F.J. Ager, M. Barbadillo Rank, F.J. Madrigal, M.A. Ontalba, M.A. Respaldiza, M.D. Ynsa, CNA: the first accelerator-based IBA facility in Spain, Nucl. Instrum. Methods Phys. Res. A 161–163 (2000) 1137–1142.
- [12] M. Mayer, SIMNRA a simulation program for the analysis of NRA RBS and ERDA, in: J.L. Duggan, I.L. Morgans (Eds.), in: Proceedings of the 15th International Conf. on the Applications of Accelerators in Research and Industry, AIP Conf. Proc., vol. 475, 1999, p. 541.
- [13] J.R. Tesmer, M.A. Nastasi, Handbook of Modern Ion Beam Analysis, Ed., Materials Research Society, 1995, p. 514.
- [14] [www-nds.iaea.org/iband1/](http://www-nds.iaea.org/iband1/).
- [15] M. Wang, G. Audi, F.G. Kondev, W.J. Huang, S. Naimi, X. Xu, The AME2016 atomic mass evaluation (II). Tables, graphs and references, Chin. Phys. C 41 (2017) 3.
- [16] J. Praena, P.F. Mastinu, M. Pignatari, J.M. Quesada, J. García López, M. Lozano, N. Dzysiuk, R. Capote, G. Martín-Hernández, Measurement of the MACS of  $^{181}\text{Ta}(n,\gamma)$  at  $kT=30$  keV as a test of a method for Maxwellian neutron spectra generation, Nucl. Instrum. Methods Phys. Res. 727 (2013) 1–6.
- [17] J. Praena, P.F. Mastinu, M. Pignatari, J.M. Quesada, R. Capote, Y. Morilla, Measurement of the MACS of  $^{159}\text{Tb}(n,\gamma)$  at  $kT=30$  keV by activation, Nucl. Data Sheets 120 (2014) 205–207.
- [18] U. Abbondanno, et al., the n\_TOF Collaboration, Nucl. Instrum. Methods Phys. Res. A 538 (2005) 692.